ISSN 1392 - 1207. MECHANIKA. 2011. 17(6): 687-691

The erosion product catcher testing in the flow of combustion products with the use of thermophoresis effect

R. Abraitis*, E. Blaževičius, D. Abraitis, S. Bočkus***, A. Čiuplys******

**Kaunas University of Technology, Tunelio 60, 44405 Kaunas, Lithuania, E-mail: rimgaudas.abraitis@ktu.lt*
***Kaunas University of Technology, Tunelio 60, 44405 Kaunas, Lithuania, E-mail: egidijus.blazevicius@ktu.lt*
****Kaunas University of Technology, Kęstučio 27, 44312 Kaunas, Lithuania, E-mail: stasys.bockus@ktu.lt*
*****Kaunas University of Technology, Kęstučio 27, 44312 Kaunas, Lithuania, E-mail: antanas.ciuplys@kru.lt*

crossref http://dx.doi.org/10.5755/j01.mech.17.6.1015

1. Introduction

Thermophoresis is the so called drift of the fractions formed in non-isothermal flow where the fractions move under the impact of temperature gradient [1]. It has a number of practical applications such as gas cleaning, prevention of fouling and corrosion in heat exchangers and turbines, semiconductor and optical waveguide manufacturing and ceramic powder production. Environmental regulations on small particles have also become more stringent due to concerns about atmospheric pollution [2-6]. Because of practical importance of thermophoresis, it has been the subject of extensive studies, both theoretical and experimental, over the years. There is a large body of papers dealing with this phenomenon [7-9]. The main parameters of thermophoresis are its velocity, mass fraction, shape and size of the particles, speed and temperature of the flow, temperature of eroding surface, eroding material, thermophoresis force and others. It should be emphasized that the vast majority of previous results, both theoretical and experimental, are for the thermophoresis of spheres. Experimental data for non-spherical particle thermophoresis have been very limited [10]. Particle size is a very important parameter of thermophoresis processes [3, 11]. The magnitude of the thermophoresis force depends on gas and particle properties as well as on temperature gradient [3].

When offering the molecular-kinetic explanation of the thermophoresis it is possible to propose that the impulse transfer to a hard fraction from the fast moving molecules with which it collides on the hot side of another fraction is stronger than from the slower moving gas molecules on the cooler side of another fraction. A moving hard fraction affected by this power is drifting through the running gas with an adequate speed of the drift [12, 13].

At the given stage of the analysis of the discussed processes it is not too important to consider the state of the particles, i.e. whether they were formed within the high-temperature flow of combustion products, fallen apart from the eroding surface and transported by the flow, or whether structural exchanges took place in the erosion products under the impact of high-temperatures. The aim of the paper is to show that even the finest fractions running in the flows of combustion products and polluting the environment are very sharp and therefore harmful rather than that they possess the fused edges as it is most frequently claimed. The goal of this study was to investigate the mass, shape and size of the erosion products of separate samples produced from different ceramic materials and to compare the experimental results with the calculation results.

2. Testing procedures

Experimental studies of the thermophoresis have been performed in the stand constructed, tested and applied to examine the erosion and ageing processes at the Institute of Architecture and Construction of Kaunas University of Technology [14]. The structural schema of the experimental setup is shown in Fig. 1. The process of thermophoresis effect in the flow of combustion products at the flow speed of 5 m/s and the flown round eroding ceramic surface heated up to 500ºC of temperature has been analysed. The particles of the erosion products together with the particles formed within the flow are transported from the eroding surface in to the erosion product catcher *1* and are fixed there. Besides, fine particle erosion products of the nanosize are also found in the erosion product catcher. Both natural and the propane/butane gases transformed into the combustion products act as energy carriers. The ceramic experimental channel constructed by the authors is a heat-resistant generator of the erosion products. The channel is hollow thick-walled inconsiderably thermoconductive equipment, in the interior cavern of which flow the formed combustion products. The height of this high-temperature channel *7* is 170 mm and its external diameter is 240 mm. It is divided into two horizontal parts, the upper *2* and the lower one *6*, the division made at 70 mm distance from the top. After having removed the upper part from the lower one, the experimental samples *4* are laid out on the plane around the mid cavern of the high-temperature channel, along which during the experiment the high-temperature flow of the combustion products will be running. The samples with dimensions of 50×300×15 mm are pressed with the upper part of the high-temperature channel and thus are fastened for the experiment. During testing the samples that are in the environment of fixed flow of the combustion products get eroded. The speed of temperature increase and decrease in the samples (in order to avoid the so called thermo-blow) and the temperature and duration of the work during the experiment are fixed with the Code-Analogue Transformer *21* within the information block *22* of the equipment. All the information about the course of the experiment is stored in the computer *PC* memory. The samples were tested in the combustion product flow for 300 min. The temperature of the flow was 800-1000°C. The area of the eroding ceramic was 0.0518 m^2. To weigh the erosion products the analytic balance ВЛА-200-М was used. The standard *Powerfire 4T* burner *8* with the thermoelement is used to work out the combustion product flow. Its normal power is 7.5 kW and gas utilization is

544 g/h. The temperature was measured with Pt-PtRh thermocouple and pyrometer Cyclops C100 *5*. The main criterion that allows to estimate erosion resistance of the tested materials is mass losses. By calculating the losses for one area unit the alterations of mass from the eroding surface area during one time unit are estimated.

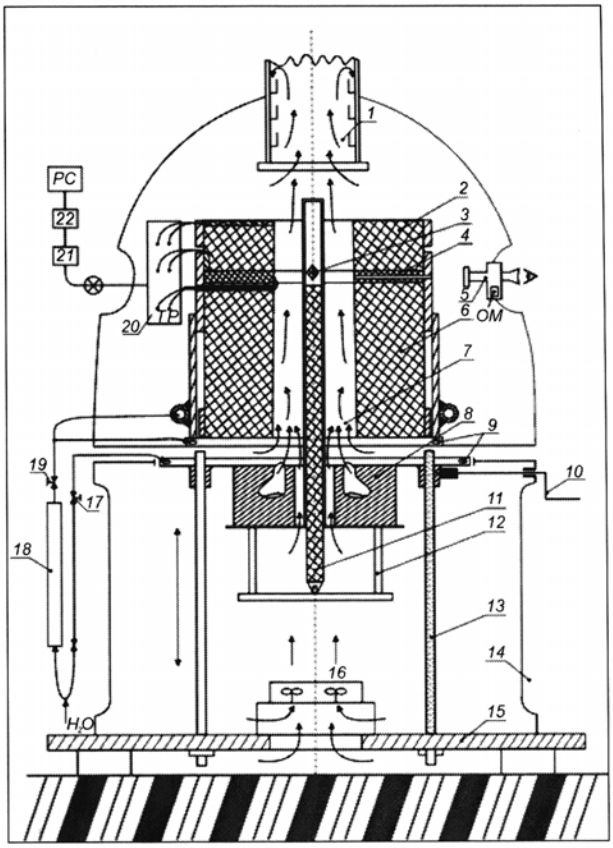

Fig. 1 Structural schema of the experimental setup [15]: *1* – erosion product catcher, *2* – upper part of the high-temperature channel, *3* – holder of samples, *4* – experimental samples, *5* – pyrometer, *6* – lower part of the high-temperature channel, *7* – channel, *8* – burner, 9 – cooled flanges, *10, 12* and *13* – knob, device and screw, respectively, for moving up or down of burner, *11* – fixing of holder, *14* – hole for circulation of air, *15* – foundation, *16* – ventilator, *17* and *19* – regulators of amount of cooling water, *18* – rotameter, *20* – panel for thermocouples connection, *21* – code-analogue transformer, *22* – information block, *PC* – computer

The interior cavern of the high-temperature channel through which the incandesced combustion products are running forms the experimental speed of the flow which is one of the test's parameters. Therefore due to the experiment's task the diameter of the cavern is changed. The erosion product catcher is fixed and fastened on the upper part of the high-temperature experimental ceramic channel, or in other words, on its top. It is produced of heat resistant stainless steel and is a construction of knots. The bottom part of the catcher which takes in the high-temperature combustion product flow with the erosion products is a hollow element fastening the catcher that holds the catcher itself. Its interior cavern is conical and its diameter may be changed from 94 mm to 110 mm. Actually, it is the bottom that determines the catcher's fixation and fastening. On this base whose external diameter is 120 mm and the height is 140 mm the collecting sections of the erosion product catcher are fixed. There are 8 sections that are fixed with the screw-thread. From these screwed sections a long hollow thin-walled cylinder is formed whose length reaches 760 mm. Within each section there are the catching volumes, i.e. the special shelves that are mounted on the interior wall. They are made of heat resistant stainless steel. During the experiments they preserve their metal surface that does not get oxidised.

We assumed that a fraction moving within the high-temperature combustion product flow is affected by the power of thermophoresis that directs the fraction to the opposite side of the temperature gradient. When affected by this power, the fraction is drifting with respect to the running high-temperature flow of combustion products at an adequate speed of the drift which, according to the molecular-kinetic theory, may be determined with the help of the following expression [8]

$$V_t = -k\frac{\nu}{T}\nabla T \tag{1}$$

where V_t is the speed of thermophoresis; k is the constant of the nondimensional thermophoresis; ν is the kinematic toughness of the high-temperature combustion products; T is the temperature of the high-temperature combustion product flow; ∇T is the difference between the sections of entering and exiting flows.

The molecular-kinetic gas theory explains the dependence of thermophoresis constant on the Knudsen number that under the free motion molecular regime approaches to 1 [13]. When considering the gas flow and gas-fraction flow as mutually intermixing flows the authors claim that if the fields of the gas flow speed ν are known, the fields of the gas-fraction flow speed may be written down as follows: $\nu+V_t$. Then the gas-fraction equation is [15]

$$\frac{\partial\varphi}{\partial t} + div\left[\varphi\left(v + V_t\right)\right] = 0 \tag{2}$$

where φ is mass density of hard fractions in the flow.

When modelling heat and mass exchange in the cavern of the high-temperature channel it is assumed that the thickness of near to wall layer of the cylindrical surface δ is considerably lower than R, i.e. the radius of the high-temperature channel cavern. Having estimated that mass concentration of the fractions in the combustion product flow is rather low (in the discussed experiments it makes no more than 3%), all the properties of the environment and flow are considered as independent on the hard fraction concentration in the high temperature combustion product flow if compared with the clean flow. When calculating the convective transmission of heat and mass with the above described assumptions the following equation is worked out [16]

$$\rho(T)C_p U_z(y,z)\frac{\partial T}{\partial z} = \lambda\frac{\partial^2 T}{\partial y^2} \tag{3}$$

where $\rho(T)$ is flow density depending on temperature; C_p is isobaric consuming content of the flow's heat; U_z expresses

the profile of the speed of the high-temperature combustion product flow depending on (y, z); λ is the coefficient of the flow's heat conductivity.

On the basis of the experimental data the thermal limit conditions are assumed as linearly decreasing in the direction of z temperatures. The assumed speed profile is the developed parabolic profile, which together with the temperature alterations undergoes the alterations in the speed amplitude. With the introduction of nondimensional variables the mathematical model of the analysed process is obtained [17]. When solving the equations of convective heat conductivity and mass exchange with the adequate limit conditions, for this variant of calculation, it is enough to find out the fraction concentration in the flow, i.e. the flow characteristics of those fractions, which under the impact of thermophoresis have a transverse power and get directed towards the catcher's wall where they are gathered in the catching volumes [18]. Other fractions are brought out and emitted from the catcher. The description of mass transmission is based on the estimation of cylindrical geometry. Then the amount of precipitated flow carriage on the walls of the catcher may be estimated as follows

$$m = GC_c^0 d_0 \tau \tag{4}$$

where G is the mass of combustion products that pass through the reactor; C_c^0 is mass concentration of fractions in the section of the flow entrance into the catcher

$$C_c^0 = \frac{\varphi_0 T_f}{\rho_f T_0} \tag{5}$$

where T_f is the temperature in the section of the flow's exit from the catcher; ρ_f is the density of the flow of the combustion products containing fractions in the section of the flow's exit from the catcher; T_0 expresses the temperature of the flow on the surface of the catcher; d is a part of the fractions carried in the flow that is precipitated on the catcher's wall; τ is the duration of the experiment; φ_0 is mass density of the fractions in the flow near the catching surface of catcher.

3. Results and discussion

The comparison of the mass of the erosion products, which were carried in the flow and caught in the catcher, and the calculated mass losses, is given in Table. The mass densities φ_0 of materials listed in Table were taken from work [19].

As we know, the profile of the flow's temperature reaches its maximum on the axis of the experimental channel's cavern. Therefore, when approaching the cooler walls of the catcher, the temperature gradient is directed toward the flow's axis. The thermophoresis power operates in opposite direction and it directs the running fractions toward the cooler walls of the catcher that are located around the high-temperature flow of combustion products. Thus the fractions in the central part of the flow are carried far away and do not enter the catching volumes. It should be noted that the precipitation efficiency of the catcher is low; nevertheless, the possibilities to increase it are rather obvious. In Fig. 2 we see a big amount of large (micronic) hard fractions and even a bigger amount of fine, i.e. the nanosized fractions. During the testing of Al_2O_3 samples in the catcher's volumes, the amount of the caught fine fractions was 2-3 times larger than the amount of big fractions. If, most possibly, among the big fractions there are the fractions that split from the stroke onto the hard surface, among the fine fractions there are partially fused and rounded surface fractions, which are fast rolling on the surface and under the impact of light air flow get lifted from the surface. The big fractions do not roll and under the impact of the light air flow do not move at all. Most probably, it is determined by the faceted character of their surface. According to Moos, the hardness of the Al_2O_3 material reaches 9.

The erosion products caught up during the testing of SiO_2 ceramic (Fig. 3) are extremely fine hard fractions that in the precipitation zone leave the traces of touching the surface. The hardness of its surface is considerably lower if compared with the Al_2O_3, ceramic and reaches only 4-5 according to Moos. Such hard fractions roll on hard surface easily and under the impact of light air flow are quickly lifted and glide in the air. As a rule, their shape is almost round.

The erosion products from $MgCr_2O_4$ oxide combinations (Fig. 4) tested in the combustion product flow are the fractions of nearly the same size. Such fractions often combine into bigger grain which, as a rule, are found on the surface of piled grain mass. The hardness of this material is 5-6 according to Moos. These erosion products roll on hard surface with difficulty and under the impact of light air flow are hardly lifted from the surface. Shapes of the fractions are most various. They are often combined with each other.

Erosion products of the crystal magnesium oxide (Fig. 5) are very sharp and split up hard grain having many splitting planes and get deteriorating easily. When entering the respiratory organs of human beings and animals, such thin long and sharp planes may be very harmful. They do not roll on the surface and under light air stream are lifted into the air with difficulty. The hardness of this material is 5-6 according to Moos.

Table

Comparison of the losses of mass m_1 of the erosion products caught in the catcher and the calculated losses m_2 (in grammes)

Section of the catcher material	Section 1		Section 2		Section 3		Section 4		Sections 5-6		Sections 7-8	
	m_2	m_1	m_2	m_1	m_2	m_1	m_2	m_1	m_2	m_1	m_2	m_1.
Al_2O_3	2.89	2.74	2.71	2.61	2.36	2.42	2.07	1.98	3.6	2.32	2.81	2.07
SiO_2	3.23	3.52	3.41	3.5	3.16	3.32	2.36	2.27	4.1	4.16	2.89	3.82
$MgCr_2O_4$	2.89	3.02	3.31	3.05	3.05	3.16	2.52	2.75	4.8	5.13	4.03	3.99
MgO	3.88	5.63	3.63	5.81	3.67	5.31	2.41	4.82	6.34	8.65	6.13	7.32

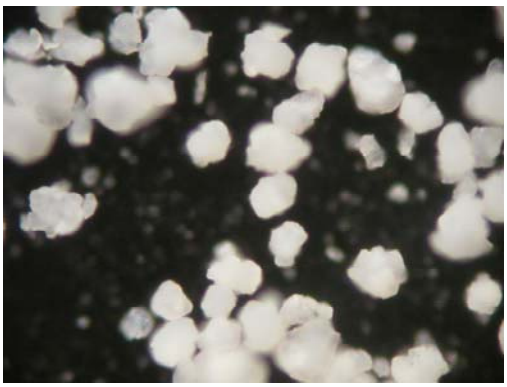

Fig. 2 Erosion products in the ceramic made of Al_2O_3, magnified ×500

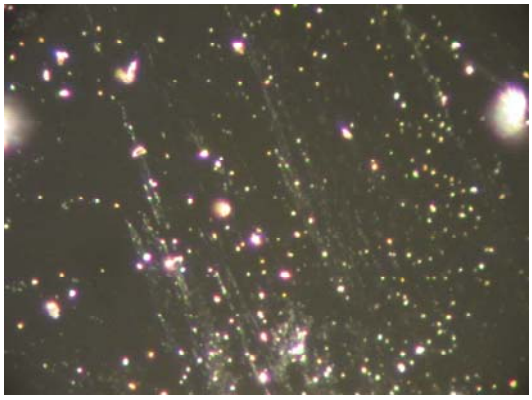

Fig. 3 Erosion products in the SiO_2 ceramic, magnified ×500

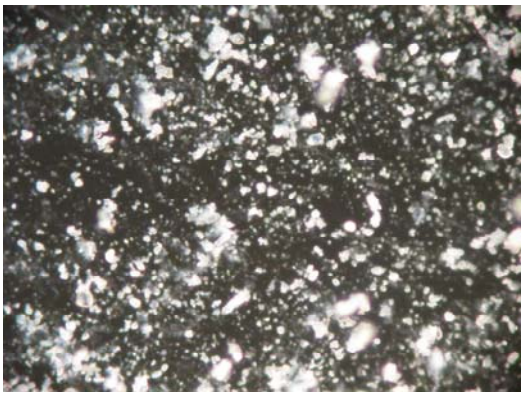

Fig. 4 Erosion products in the $MgCr_2O_4$ ceramic, magnified ×500

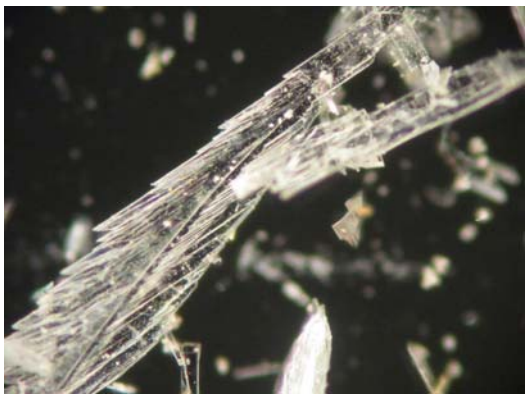

Fig. 5 Erosion products in the MgO crystal ceramic, magnified ×500

It is important to stress that during the discussed processes the newly formed products from the eroding surface and the flow materials have been observed. This has been determined by the temperature gradient found between the temperature of the combustion product gas flow and the surface temperature of the erosion product catcher due to the mass exchange laws. In the discussed experiment it is not as much important of what group the micro- and nanofractions are or what their amount is. It is significant that such a process has been observed and that it may be fixed. The use of this process to control the erosion products and their operation is very significant for the determination of everyday pollution of natural environment with the thrown out hard fractions [18, 20].

4. Conclusions

1. It has been demonstrated that the drift phenomenon known as thermophoresis actively affects the hard ceramic fractions in nonisothermal combustion product flow, which may be precipitated on a cool wall when an adequate temperature gradient is formed on the fraction's surface.

2. On the basis of the above mentioned observation the erosion product catcher has been constructed in which it is possible to collect the fine and bigger erosion products and the hard fractions that are formed in the flow.

3. In various types of ceramics the erosion products differ in their shape, volume and reaction to the thermophoresis effect. The calculations showed that the efficiency of the catcher's precipitation reaches around 12-15% of the pointed out mass of an eroding surface.

4. It was found out that the efficiency of fraction precipitation had not been properly investigated. The analysis has confirmed that this process extends a considerable potential resource for the efficiency increase thus seeking to diminish the environmental pollution with the hard fractions as combustion waste.

References

1. **Kandasamy, R.; Hayat, T.; Obaidat, S.** 2011. Group theory transformation for Soret and Dufour effects on free convective heat and mass transfer with thermophoresis and chemical reaction over a porous stretching surface in presence of heat source/sink, Nuclear Engineering and Design 241: 2155-2161.

2. **Wang, X.; You, C.; Liu, R.; Yang, R.** 2011. Particle deposition on the wall driven by turbulence, thermophoresis and particle agglomeration in channel flow, Proceedings of the Combustion Institute 33: 2821-2828.

3. **Sohn, Y.M.; Baek, S.W.; Kim, D.Y.** 2003. Thermophoresis of particles in gas-particle two-phase flow with radiation effect, Numerical Heat Transfer, Part A 41: 165-181.

4. **Dong, Y-H.; Chen, L-F.** 2011. The effect of stable stratification and thermophoresis on fine particle deposition in a bounded turbulent flow, International Journal of Heat and Mass Transfer 54: 1168-1178.

5. **Daunys, M.; Dundulis, R.; Karpavičius, R.; Bortkevičius, R.** 2011. Aging investigation of metals of the pipes in Lithuanian Powder Station, Mechanika 1(17): 13-20.

6. **Kaliatka, T.; Marao, A.; Karalevičius, R.; Ušpuras, E.; Kaliatka, A.** 2011. Best estimate analysis of processes in RBMK fuel rods during the operation cycle, Mechanika 4 (17): 387-394.

7. **Goren, S.L.** 1977. Thermophoresis of aerosol particles in the laminar boundary layer on a flat plate, Journal of Colloid and Interface Science 61: 77-85.

8. **Talbot, R.K.; Cheng, R.W.; Schefer, D.R.; Wilis, D.R.** 1980. Thermophoresis of particles in a heated boundary layer, Journal of Fluid Mechanics 4(101): 737-758.

9. **Hong, K.; Kang, S.** 1988. Three-dimensional analysis of heat transfer and thermophoresis particle deposition in OVD process, International Journal of Heat and Mass Transfer 41: 1339-1346.

10. **Zheng, F.** 2002. Thermophoresis of spherical and non-spherical particles: a review of theories and experiments, Advances in Colloid and Interface Science 97: 255-278.

11. **Shah, K.V.; Cieplik, M.K.; Bertrand, C.I.; Kamp, W.L.; Vuthaluru, H.B.** 2010. A kinetic-empirical model for particle size distribution evolution during pulverised fuel combustion, Fuel 89: 2438-2447.

12. **Amel'kovich, Yu. A.; Astankova, A.P.; Tolbanova, L.O.; Il'in, A.P.** 2007. Synthesis of titanium and zirconium nitrides by burning mixtures of their oxides with aluminum nanopowder and air, Refractories and Industrial Ceramics 6(48): 425-428.

13. **Pivinskii, Yu.E.** 2007. Nanodisperse silica and some aspects of nanotechnologies and the field of silicate materials science. Part 2, Refractories and Industrial Ceramics 6(48): 435-443.

14. **Abraitis, R.; Abraitis, D.; Blaževičius, E.; Goberis, S.** 2010. Investigation of erosion and ageing processes in high-temperature building materials under the impact of combustion product stream, Energetika 3-4 (56): 238-246. (in Russian).

15. **Landau, L.D.; Lifshitz, E.M.** 1987. Fluid Dynamics, London: Pergamon. 321p.

16. **Petuchov, B. S.** 1967. Heat Transfer and Friction in Laminar Flow of Fluid in Tubes. Moscow: Energija. 287p. (in Russian).

17. **Sebisi, T.; Bredshou, P.** Convective Heat Transfer. Moscow, Mir, 1987. 418 p.

18. **Krasnyi, B.L., Tarasovskii, V.P.** 2007. Risks of nanotechnologies for human health and environment, Steklo i Keramika 1 (32): 17-22 (in Russian).

19. **Goberis, S.; Antonovič, A.** 2007. Fireclay Refractory Concrete. Vilnius: Technika, 360p. (in Lithuanian).

20. **Pivinskii, Yu. E.** 2007. Scientific research and development of nanodisperse silica and some aspects of nanotechnologies in the field of silicate materials science. Part 1, Refractories and Industrial Ceramics 6(48): 408-416.

R. Abraitis, E. Blaževičius, D. Abraitis, S. Bočkus, A. Čiuplys

EROZIJOS PRODUKTŲ GAUDYKLĖS TYRIMAI DEGIMO PRODUKTŲ SRAUTE PANAUDOJANT TERMOFOREZO EFEKTĄ

R e z i u m ė

Mažai tirtas termoforezo reiškinys turi svarbią reikšmę eilėje technologinių procesų, ypač energetikoje ir cheminėje pramonėje. Erozijos produktų kontrolė ir analizė turi didelę reikšmę nustatant kasdieninį gamtos užteršimą išmetosiomis kietosiomis dalelėmis į mūsų gyvenimo aplinką. Tai gali turėti neigiamą poveikį žmogaus organizmui, ypač kvėpavimo organams.

Straipsnyje pateikti bandinių, pagamintų iš skirtingų keraminių medžiagų, erozijos proceso eksperimentinių tyrimų rezultatai. Bandiniai buvo tiriami specialiame autorių sukonstruotame stende. Nustatyta skirtingų bandinių erozijos produktų masė, forma ir matmenys. Buvo palygintas masių skirstinys, gautas skaičiavimo būdu ir eksperimentiniu tyrimu. Atkreipiamas dėmesys į aštrius ir briaunotus erozijos produktus.

R. Abraitis, E. Blaževičius, D. Abraitis, S. Bočkus, A. Čiuplys

THE EROSION PRODUCT CATCHER TESTING IN THE FLOW OF COMBUSTION PRODUCTS WITH THE USE OF THE THERMOPHORESIS EFFECT

S u m m a r y

The unextensively examined phenomenon of thermophoresis plays an important role in a number of technological processes, especially in energetics and chemistry industry. Control and analysis of the erosion products is very significant for the determination of everyday pollution of natural environment with the hard fractions that are emitted into the environment and may have a harmful effect on a human organism, especially on the respiratory organs. This paper presents the results of experimental investigation of the erosion process of samples produced from different ceramic materials. The samples were tested in a special stand constructed by the authors. The mass, shape and size of the erosion products of separate samples were investigated. Particle mass distributions from calculation and experiment were compared. The paper considers the sharp and faceted products of erosion.

Received February 11, 2011
Accepted November 30, 2011